Journal of the Korean Magnetic Resonance Society **2021**, *25*, 51-57
DOI 10.6564/JKMRS.2021.25.4.051

Cyclotron Resonance Line Widths in Wurtzite ZnO Structure under Circularly Oscillating Fields

Jung-Il Park*

Nano-Physics and Technology Laboratory, Department of Physics, Kyungpook National University, Daegu 41566, Republic of Korea

Received Nov 29, 2021; Revised Dec 14, 2021; Accepted Dec 17, 2021

Abstract We study optical quantum transition line widths in relation to magnetic field dependence properties of the electrons confined in an infinite square well potential system between $z = 0$ and $z = L_z$ in the $z-$ direction. We consider two systems-one is subject to right circularly oscillating external fields and the other is subject to left circularly oscillatory external fields. Our results indicate that the line widths of right circularly oscillating external fields is larger than the line widths of left, while the opposite result is obtained for the line widths.

Keywords Cyclotron resonance, line widths, absorption power, scattering factor function, wurtzite structure

Introduction

There has been a great deal of interest in zinc oxide (ZnO) semiconductor materials lately, as seen from a surge of a relevant number of publications. The interest in ZnO is fueled and fanned by its prospects in optoelectronics applications owing to its direct wide band gap (E_g ~ 3.3 eV at 300 K).[1–2] Most of the group Ⅱ-Ⅵ binary compound semiconductors crystallize in either hexagonal wurtzite or cubic zinc-blende structure where each anion is surrounded by four cations at the corners of a tetrahedron, and vice versa. This tetrahedral coordination is typical of sp^3 covalent bonding, but these materials also have a substantial ionic character. ZnO is a Ⅱ-Ⅵ compound semiconductor whose iconicity resides at the borderline between covalent and ionic semiconductor. We have considered two systems-one is under a right circularly oscillating external fields (RCF) and the other is under a left circularly oscillating fields (LCF). The main purpose of this work is to compare cyclotron transition line widths (CTLWs) under both directions right and left of circularly polarized oscillating external fields. There are several methods to obtain CTLWs in response function. Among them the theoretical and experimental investigations in the presence of very high electric and/or magnetic fields have received special attention. The theoretical studies performed so far on high electric field transport are usually based on the following methods: the Green's function approach, Feynman's path integral approach, the Wigner representation approach, and the equilibrium average projection scheme (EAPS). Despite the fact that all these methodologies are quite reasonable, the nonlinear behavior has been investigated in limited schemes. Actually, for a more acceptable interpretation of the transport behavior of electrons which are subject to strong electric fields.[3–9] In this study, through a numerical calculation of the theoretical result, we investigated the magneto-optical cyclotron resonance in wurtzite structure (in Fig. 1). We first modify the EAPS formula into one that is easy to deal with. Next, we calculate the magnetic field dependence of the CTLWs and the absorption power of ZnO for

* Address correspondence to: **Jung-Il Park**, Department of Physics, Kyungpook National University, 80 Daehak-ro, Buk-gu, Daegu 41566, Republic of Korea. Tel: 82-53-950-5316; E-mail: jipark@knu.ac.kr

$\lambda = 220,\ 394,\ 513,\ 550,\ 720\ \mu\mathrm{m}$ at $\mathrm{T} = 50\ \mathrm{K}$.

Theory

When a static magnetic field $\vec{B} = B\hat{z}$ is applied to an electron system, the single electron energy state is quantized to the Landau levels. We select a system of electrons confined in an infinite square well potential between $z = 0$ and $z = L_z$ in the $z-$direction. Using the Landau gauge $\vec{A} = (0, B_x, 0)$, [10–17] we define a single electron Hamiltonian h_e as

$$h_e = -\frac{\hbar^2}{2m}\left[\nabla^2 + 2i\left(\frac{eB}{\hbar}\right)x\frac{\partial}{\partial y} - \left(\frac{eB}{\hbar}\right)^2 x^2\right] + U(\mathrm{z}), \qquad (1)$$

and we obtain the eigenstate in the system as

$$\Psi_{N_\alpha,k_y,k_z}(x,y,z) \equiv |\alpha\rangle = \tilde{C}_G \tilde{\phi}_{kr}^{(plw)} \tilde{\phi}_{N_\alpha}(x_l)\tilde{\Phi}_{n_\alpha}^{(cfn)}(z), \quad (2)$$

where the plane wave is $\tilde{\phi}_{kr}^{(plw)} \equiv \exp(ik_y y)$ and the explicit function is

$$\tilde{\phi}_{N_\alpha}(x_l) = \tilde{\mathrm{N}}_r \exp\left(-\frac{x_l^2}{2l_0^2}\right) H_{N_\alpha}\left(\frac{x_l}{l_0}\right). \qquad (3)$$

Here, $H_{N_\alpha}(x)$ is the Hermite polynomials function, $l_0 = \sqrt{\hbar/eB}$ is the radius of cyclotron motion, $\omega_c = eB/m_e^*$ is the cyclotron frequency, m_e^* is the effective mass of the electron, $x_\alpha = -\hbar k_{z\alpha}/eB = -\hbar k_{z\alpha}/m_e^*\omega_0$ is the center of cyclotron motion, and $x_l \equiv x - x_\alpha$. The confined wave function is

$$\tilde{\Phi}_{n_\alpha}^{(cfn)}(z) = \begin{cases} \dfrac{1}{\sqrt{(z_0/2) + (1/\kappa_{n_\alpha})}} \sin\left(k_{n_\alpha} z\right), & (0 \le z \le z_0) \\ \dfrac{1}{\sqrt{(z_0/2) + (1/\kappa_{n_\alpha})}} \exp\left[\kappa_{n_\alpha}(z - z_0)\right], & (z_0 \le z), \end{cases} \qquad (4)$$

where κ_{n_α} and k_{n_α} (the quantization condition for the z-direction components of the electron wave vector of κ and k, respectively) are obtained by solving the simultaneous equations $\kappa = -k\cot kz_0$ and $\kappa + k = 2m_e^* U_0/\hbar$, with the conditions $0 < \kappa$ and $0 < k$. Here, the square-well confinement potential $U(z) \equiv U_0$ is a constant potential in the region $0 < z < z_0$, and $U(z) \equiv \infty$ is a constant potential in the region $z < 0$, $z_0 < z$. The values of normalization factors are $\tilde{C}_G \equiv 1/\sqrt{L_y}$, $\tilde{N}_r \equiv 1/\sqrt{\left(\sqrt{\pi}2^N N!\, l_0\right)}$. The values of normalization factors change in other systems. We obtain the corresponding eigenvalue as follows:

$$\varepsilon_{N_\alpha,n_\alpha,k_{y\alpha},k_{z\alpha}} = \left(N_\alpha + \frac{1}{2}\right)\hbar\omega_c + n_\alpha^2 \frac{\hbar^2\pi^2}{2m_e^* L_{z(\mathrm{sys})}^2} \qquad (5)$$

$\left(N_\alpha = 0,1,2,3,.....n_\alpha = 0,1,2,3,...\right)$.

Here, $L_{z(\mathrm{sys})}^2 \equiv z$ is the size of materials in the z-direction. If we consider a system of many bodies that are subject to circularly polarized oscillatory external fields $E_+(t) = E_0\exp(i\omega t)$, where ω is the angular frequency, then, using the Coulomb gauge $\vec{E}(t) = -\partial\vec{A}/\partial t$, the total Hamiltonian of the system is $H(t) = H_s + H'(t) = H_s + \left(-i/\omega\right)J^+E_+(t)$. The many-electron current operator $J^\pm$ are defined as

$$J^+ = \sum_\alpha j_\alpha^+ a_{\alpha+1}^\dagger a_\alpha \qquad (6)$$

and

$$J^- = \sum_\beta (j_\beta^+)^* a_\beta a_{\beta+1}, \qquad (7)$$

where $J^\pm = J_x \pm iJ_y$ are the two components of the single electron current operator j, the matrix elements are

$$j_\beta^+ \equiv \sum_\beta \left\langle \beta+1 \middle| j^+ \middle| \beta \right\rangle = \tilde{g}_{(\mathrm{sys})} \sum_\beta \sqrt{\left(N_\beta + 1\right)_\beta}, \qquad (8)$$

and

$$j_\beta^- \equiv \sum_\beta \left\langle \beta \middle| j^+ \middle| \beta+1 \right\rangle = \tilde{g}_{(\mathrm{sys})} \sum_\beta \sqrt{N_\beta}, \qquad (9)$$

where $\tilde{g}_{(\mathrm{sys})} \equiv \left(-ie\hbar/m_e^*\right)\sqrt{1/l_0^2}$. $\tilde{g}_{(\mathrm{sys})}$ can be changed for other systems and external fields. Here, $a_1(a_2^\dagger)$ is the annihilation operator (creation operator) of a fermion and $\langle\beta|(\langle\alpha|)$ is the eigenstate of a single electron. We define the Hamiltonian of the electron-phonon interacting system as

$$H_s = H_e + H_p + V$$
$$= \sum_\alpha \langle\alpha|h_e|\alpha\rangle a_\alpha^\dagger a_\alpha + \sum_q \hbar\omega_q b_q^\dagger b_q + \sum_q \sum_{k,\lambda} C_{k,\lambda}(q) a_k^\dagger a_\lambda (b_q + b_{-q}^\dagger), \qquad (10)$$

where, H_e is the electron Hamiltonian, H_p is the phonon Hamiltonian and V is the

electron-piezoelectric phonon interaction Hamiltonian. The $b_1(b_2^\dagger)$ is the annihilation operator (creation operator) of boson particles, and $\vec{q}$ is the phonon wave vector. The interaction Hamiltonian of the electron-piezoelectric phonon scattering system is V, where the coupling matrix element of the electron-phonon interaction $C_{k,\lambda}(q)$ is $C_{k,\lambda}(q) \equiv |V_q|^2 \langle k|\exp(i\vec{q}\cdot\vec{r})|\lambda\rangle$, and $\vec{r}$ is the position vector of electrons. Following Meijer and Polder, we adopted the isotropic interaction formalism to choose the interaction factor V_q is given by

$$|V_q|^2 = \frac{\bar{K}^2 \hbar v_s e^2}{2\chi\varepsilon_0\Omega}\frac{1}{q}. \quad (11)$$

Here the $\bar{K}$ is the electrochemical constant, the v_s is the sound velocity in solid, the Ω is the volume of the system, the ε_0 is the permittivity of free space and the χ is the dielectric constant. The Fermi-Dirac distribution functions are $f_\alpha = 1/[e^{\varepsilon_\alpha/k_BT}+1]$ and $f_\beta^{\pm} = 1/[e^{\varepsilon_\beta^{\pm}/k_BT}+1]$, in which the eigenvalues are

$$\varepsilon_\alpha = \left[\left(N_\alpha + \frac{1}{2}\right)\hbar\omega_c + \frac{\hbar^2 k_{z\alpha}^2}{2m^*} + (\varepsilon_c - \varepsilon_F)\right], \quad (12)$$

$$\varepsilon_\beta^{\pm} = \left[\left(N_\beta + \frac{1}{2}\right)\hbar\omega_c + \frac{\hbar^2 k_{z\beta}^2}{2m^*} + (\varepsilon_c - \varepsilon_F)\right]\delta_{k_\beta, k_\beta \pm q_{yz}} \quad (13)$$

$$= \left[\left(N_\beta + \frac{1}{2}\right)\hbar\omega_c + \frac{\hbar^2 (k_{z\alpha} \pm q_z)^2}{2m^*} + (\varepsilon_c - \varepsilon_F)\right], \quad (14)$$

where $k_{z\alpha}$ is the z component of the electron wave vector and the chemical potential energy:

$$\varepsilon_c - \varepsilon_F(T) = 0.5\left[\varepsilon_g(T) - \frac{kT}{T-\xi} - \frac{3}{4}k_BT\ln\left(\frac{\bar{m}}{m^*}\right)\right], \quad (15)$$

where ε_c is the conduction band minimum energy, $\varepsilon_F(T)$ is the Fermi energy, $\varepsilon_g(T)$ is the band gap energy at T, k and ξ are the characteristic constant of the materials, and $\bar{m}$ is the density of states effective mass of hole. The phonon distribution parts are $N_q^- = \langle b_q^\dagger b_q\rangle = n_q$ and $N_q^+ = \langle b_q b_q^\dagger\rangle = n_q + 1$, where the Bose-Einstein distribution function is $n_q = [e^{\varepsilon(q,T)} - 1]^{-1}$. Here the phonon energy is

$$\varepsilon(q,T) = \frac{\hbar\omega_q}{k_BT} = \frac{\hbar v_s}{k_BT}\sqrt{\left(q_{\perp n}^{\mp k\lambda}\right)^2 + q_z^2}. \quad (16)$$

This result can be applied directly to the numerical analysis through wave vector integration.

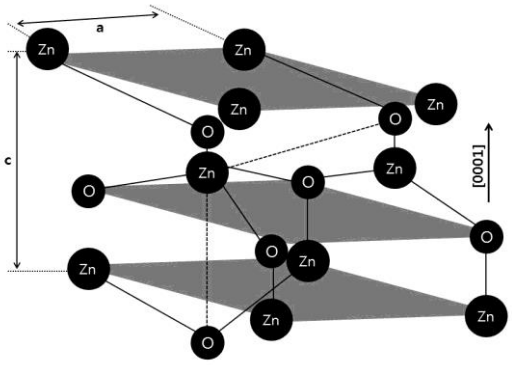

Figure 1. Schematic representation of a wurtzitic ZnO structure having lattice constants a in the basal plane and c in the basal direction.

Absorption Power Formula and Line Widths

We suppose that an oscillatory electric field $E(t) = E_0\exp(i\omega t)$ is applied along the $z-$axis, which gives the absorption power delivered to the system as $P_{abs}(\omega) = (E_0^2/2)\,\mathrm{Re}\{\sigma(\omega)\}$. In this equation, "Re" is the real component and $\sigma(\omega)$ is the magneto-optical conductivity tensor, which is the coefficient of the current formula. In order to apply the linear response formula to optical quantum transition system, in a RCF system, we replace r_k with $J_k \equiv J^-$, L_l'X with $L_l\text{'X} \equiv (-i/\omega)\left[J^+, X\right]$, and $J_l \equiv J^+$ for current system under an oscillating external field of the frequency ω. We obtain the right circular current from the response formula,

$$\mathrm{J}^R(\omega) = \left[\frac{(-i/\hbar)\Lambda_{kl}^{(R)}}{\omega - A_{kl}^{(R)} + \Xi_{kl}^{(R)}(\omega)}\right]\mathrm{E}(\omega), \quad (17)$$

where

$$\Lambda_{kl}^{(R)} = -\left[\left(\frac{i}{\omega}\right)\sum_\alpha j_{\alpha+1,\alpha}^+ j_{\alpha,\alpha+1}^+ (f_{\alpha+1} - f_\alpha)\right], \quad (18)$$

$$\Lambda_{kl}^{(R)} = i\omega_c. \tag{19}$$

We can easily obtain the LFC from the response formula with the EAPS, while recent research on the response formula was restricted to the right circular current under a right circular polarized external field. For the left circular polarized external system, we replace r_k to $J_k \equiv J^+$, L_l'X with $L_l\text{'X} \equiv (-i/\omega)\left[J^-, X\right]$, and $J_l \equiv J^-$. We obtain the left circular current from the response formula as

$$\mathrm{J}^L(\omega) = \left[\frac{(-i/\hbar)\Lambda_{kl}^{(\mathrm{L})}}{\omega - A_{kl}^{(\mathrm{L})} + \Xi_{kl}^{(\mathrm{L})}(\omega)}\right]\mathrm{E}(\omega), \tag{20}$$

where

$$\Lambda_{kl}^{(\mathrm{L})} = -\left[\left(\frac{i}{\omega}\right)\sum_{\alpha} j_{\alpha+1,\alpha}^{+} j_{\alpha,\alpha+1}^{+}\left(f_{\alpha+1} - f_{\alpha}\right)\right], \tag{21}$$

and

$$\Lambda_{kl}^{(\mathrm{L})} = -i\omega_c. \tag{22}$$

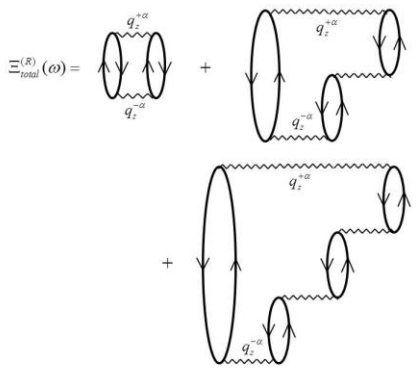

Figure 2. Ring contribution to the scattering factor function.

The scattering factor function, $\Xi_{kl}^{(R)}(\omega)\left[\Xi_{kl}^{(\mathrm{L})}(\omega)\right]$, is expressed in the complex form as $\Xi_{kl}^{(R)}(\omega) \equiv i\Delta_{total}^{(R)} + \Gamma_{total}^{(R)}(\omega)$, where $\Delta_{total}^{(R)} = \mathrm{Im}\,\Xi_{total}^{(R)}(\omega)$, giving the line shift of a response formula, and $\Gamma_{total}^{(R)}(\omega) = \mathrm{Re}\,\Xi_{total}^{(R)}(\omega)$ giving the line width of the response formula. The scattering factor function is schematically represented in Fig. 2. In most cases, the imaginary part of the scattering factor, $\Delta_{total}^{(R)}$, is negligible in a real system because of its small value. We obtain final result of the absorption power formula, in right circularly oscillating external fields, [18–19]

$$P^{(R)}(\omega) \propto \left(\frac{e^2\omega_c^2}{\pi^2\hbar\omega}\right)\left\{\frac{\Gamma_{total}^{(R)}(\omega_c)\sum_{N_\alpha}\int_{-\infty}^{+\infty} dk_{z\alpha}(N_\alpha+1)(f_\alpha - f_{\alpha+1})}{(\omega-\omega_c)^2 + \left[\Gamma_{total}^{(R)}(\omega_c)\right]^2}\right\}. \tag{23}$$

Here, the scattering factor function is given by

$$\Gamma_{total}^{(R)}(\omega) = \mathrm{Re}\,\Xi_{kl}^{(R)}(\omega) = \sum_{\mp}\sum_{N_\alpha=0}\sum_{N_\beta=0}\Gamma_{\alpha,\beta}^{(R)\mp}$$

$$= \left(\frac{\Omega}{4\pi\hbar^2 v_s}\right)\left(\frac{\pi}{L_z}\left(2+\delta(n_\alpha,n_\beta)\right)\right)\left\{\frac{\sum_{\mp}\sum_{N_\alpha=0}\sum_{N_\beta=0}\int_{-\infty}^{+\infty} dk_{z\alpha}\int_{-\infty}^{+\infty} dq_z Y_{\alpha,\beta}^{(R)\mp}}{\sum_{N_\alpha=0}\int_{-\infty}^{+\infty} dk_{z\alpha}(N_\alpha+1)(f_{\alpha+1}-f_\alpha)}\right\}. \tag{24}$$

Because the integrand factors $Y_{\alpha,\beta}^{(R)\mp}$ are in a complex form, we arrange them in the appendix. For the left circularly oscillating external fields, we obtain final result of the absorption power formula,

$$P^{(\mathrm{L})}(\omega) \propto \left(\frac{e^2\omega_c^2}{\pi^2\hbar\omega}\right)\left\{\frac{\Gamma_{total}^{(\mathrm{L})}(\omega_c)\sum_{N_\alpha}\int_{-\infty}^{+\infty} dk_{z\alpha}(N_\alpha+1)(f_\alpha - f_{\alpha+1})}{(\omega-\omega_c)^2 + \left[\Gamma_{total}^{(\mathrm{L})}(\omega_c)\right]^2}\right\}. \tag{25}$$

$$\Gamma_{total}^{(\mathrm{L})}(\omega) = \mathrm{Re}\,\Xi_{kl}^{(\mathrm{L})}(\omega) = \sum_{\mp}\sum_{N_\alpha=0}\sum_{N_\beta=0}\Gamma_{\alpha,\beta}^{(\mathrm{L})\mp}$$

$$= \left(\frac{\Omega}{4\pi\hbar^2 v_s}\right)\left(\frac{\pi}{L_z}\left(2+\delta(n_\alpha,n_\beta)\right)\right)\left\{\frac{\sum_{\mp}\sum_{N_\alpha=0}\sum_{N_\beta=0}\int_{-\infty}^{+\infty} dk_{z\alpha}\int_{-\infty}^{+\infty} dq_z Y_{\alpha,\beta}^{(\mathrm{L})\mp}}{\sum_{N_\alpha=0}\int_{-\infty}^{+\infty} dk_{z\alpha}(N_\alpha+1)(f_{\alpha+1}-f_\alpha)}\right\}. \tag{26}$$

We also arrange $Y_{\alpha,\beta}^{(\mathrm{L})\mp}$ in the appendix.

Results

For that purpose we calculated the LWs for ZnO which is a typical wurtzite material. Note that, since the theory was proved to be valid for an infinite square well potential, if it gives good interpretation for wurtzite materials. Through the numerical calculation of Eq. (23) and Eq. (24), we analyzed LWs in ZnO. We use $m^* = 0.27m_0$ and $\bar{m} = 1.8m_0$, which are the effective masses of constants of ZnO are $\rho = 4.09\times10^3\ \mathrm{kg/m^3}$,

$v_{sl} = 5.61\times10^{3}$ m/s is the longitudinal sound velocity, $v_{st} = 2.99\times10^{3}$ m/s is the transverse sound velocity, $k = 1.78\times10^{-3}$ eV/K, $\xi = 204$ K and $|K|^2 = 6.27\times10^{-2}$. The speed of sound v_s in Eq. (16) is replaced by the average value v_s of v_{sl} and v_{st}, as $\bar{v}_s = (v_{sl} + v_{st})/2$ and the energy gap $\varepsilon_g(T)$ is replaced by $\bar{\varepsilon}_g = 3.42$ eV as an approximation, noting that the variation with the temperature is very small. A more accurate value of $\varepsilon_g(T)$ can be obtained by Eq. (15) if the characteristic constants k and ξ are available.

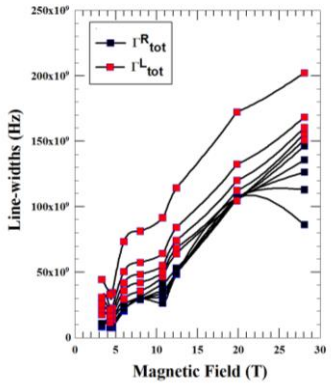

Figure 3. The magnetic field dependence of line widths, $\Gamma^{(R)}(B)$ and $\Gamma^{(L)}(B)$ of ZnO for $\lambda = 220$, 394, 513, 550, 720 μm at T = 50 K.

In Fig. 3, we show the obtained magnetic field dependence of the LWs, $\Gamma(B)$ of ZnO, at T = 55, 60, 65, 70, and 80 K. The results indicate that $\Gamma^{(L)}(B)$ is larger than $\Gamma^{(R)}(B)$ at all temperatures. The result is also able to reasonable explain the directional characteristic of electron motion, which is given by the magnetic field direction and the condition of the system. The analysis of the magnetic fields dependence of LWs in various magnetic fields is very important for understanding the magnetic properties of materials. The analysis of the magnetic field dependence of LWs is very difficult using other theories or in experiments, because it is necessary to calculate or observe absorption power at various external field wavelengths. The EAPS theory has an advantage because we can directly obtain LWs, through EAPS, at various external field wavelengths. We do not need to calculate absorption power to obtain LWs. In order to analyze the quantum transition process in the case of the RCF, we denote the total LWs as

$$\Gamma^{(R)}_{total} \equiv \Gamma(T)^{(R)}_{\mathrm{int}raL} + \Gamma(T)^{(R)}_{\mathrm{int}erL},$$

where

$$\Gamma^{(R)}_{\mathrm{int}raL} \equiv \Gamma(T)^{(R)\mathrm{em}}_{\mathrm{int}raL} + \Gamma(T)^{(R)\mathrm{ab}}_{\mathrm{intra}L},$$

and

$$\Gamma^{(R)}_{\mathrm{inter}L} \equiv \Gamma(T)^{(R)\mathrm{em}}_{\mathrm{inter}L} + \Gamma(T)^{(R)\mathrm{ab}}_{\mathrm{inter}L},$$

are the LWs of the total intra-level and total inter-level transition process, respectively. Here,

$$\Gamma(T)^{(R)\mathrm{em}}_{\mathrm{int}raL} \equiv \Gamma^{(R)+}_{0,0},$$

$$\Gamma(T)^{(R)\mathrm{em}}_{\mathrm{inter}L} \equiv \Gamma^{(R)+}_{0,1},$$

$$\Gamma(T)^{(R)\mathrm{ab}}_{\mathrm{int}raL} \equiv \Gamma^{(R)-}_{0,0},$$

and

$$\Gamma(T)^{(R)\mathrm{ab}}_{\mathrm{inter}L} \equiv \Gamma^{(R)-}_{0,1}$$

are the LWs of the intra-level emission transition, the inter-level emission transition process, the intra-level absorption transition and the inter-level absorption process, respectively.

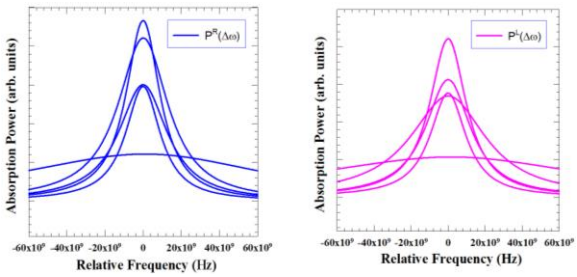

Figure 4. The relatively frequency $\Delta(\omega)$ dependence of the absorption power, $P^{(R)}(\Delta\omega)$ and $P^{(L)}(\Delta\omega)$ of ZnO for $\lambda = 220$, 394, 513, 550, 720 μm at T = 50 K.

In Fig. 4, the relatively frequency $\Delta(\omega)$ dependence of the absorption power, $P^{(R)}(\Delta\omega)$ and $P^{(L)}(\Delta\omega)$ of ZnO, with $\lambda = 220$, 394, 513, 550, 720 μm at T = 50 K are shown. From the graph of $P^{(R)}(\Delta\omega)$ and $P^{(L)}(\Delta\omega)$, we can see the broadening effects near the resonance peak for

various external fields. The relativity frequency $\Delta(\omega)$ dependence of absorption power represents the magnetic field dependence property of absorption power, which is given by external field wavelength and the condition of the system. In addition, the advantages of the EAPS theory are evident in the calculation of LWs for various cases. The results indicate that the EAPS is useful to explain the resonant phenomena based on the quantum transition and the scattering effects in a microscopic view.

Summary

As a summary, the EAPS theory provides a relatively easy approach to the analysis of the magnetic field dependence of the LWs. Furthermore, we found that LWs of ZnO increased with the temperature. We also found that $\Gamma^{(L)}(B)$ is larger than $\Gamma^{(R)}(B)$ at all temperatures. The result is able to reasonable explain the directional characteristic of electron motion, which is given by the magnetic field direction and the condition of the system. Therefore, we predict that this result was because of the geometrical structure of wurtzite type semiconductors.

Appendix: Integrand of the scattering factor function

In continuous approximation, the interaction matrix part in an infinite square well potential system is given as

$$\left[C_{\mathrm{N}_\alpha,\mathrm{N}_\beta}(q)C_{\mathrm{N}_\beta,\mathrm{N}_\alpha}(q)\right]^{\mp} \equiv \left|V_q\right|^2 K_{\beta,\alpha}^{\alpha,\beta}(t)\left|F_{\alpha,\beta}(q)\right|^2 \delta_{k_{\beta z},k_{\alpha z}\pm q_z},$$

$$\left[C_{\mathrm{N}_\beta,\mathrm{N}_\alpha}(q)C_{\mathrm{N}_\alpha,\mathrm{N}_\beta}(q)\right]^{\mp} \equiv \left|V_q\right|^2 K_{\alpha,\beta}^{\beta,\alpha}(t)\left|F_{\alpha,\beta}(q)\right|^2 \delta_{k_{\beta z},k_{\alpha z}\mp q_z},$$

if $N_\alpha < N_\beta$ and $N_k < N_\lambda$, the K-matrix is

$$K_{k,\lambda}^{\alpha,\beta} \equiv \sqrt{\frac{N_\alpha!}{N_\beta!}}\sqrt{\frac{N_k!}{N_\lambda!}}\left(\sqrt{t}\right)^{N_\beta-N_\alpha}\left(\sqrt{t}\right)^{N_\lambda-N_k}\exp(-t)L_{N_\alpha}^{N_\beta-N_\alpha}(t)L_{N_k}^{N_\lambda-N_k}(t),$$

where the Legendre function is

$$L_n^m(t) = \frac{1}{(n!)}\exp(t)\frac{1}{t^m}\left(\frac{d^n}{dt^n}\right)\left[t^{n+m}\exp(-t)\right]$$

$$t \equiv \frac{r_0^2\left(q_x^2+q_y^2\right)}{2}.$$

The matrix element of the confinement potential is

$$\left|F_{\beta,\alpha}(q)\right|^2 = \left|\int_{-\infty}^{+\infty}\phi_\beta^{cfn}(z)\exp(\mathrm{i}q_z z)\phi_\alpha^{cfn}(z)\,\mathrm{d}q_z\right|^2$$

Then, through continuous approximation, we derived the integrand of the scattering factor

$$Y_{\alpha,\beta}^{(R)\mp} \equiv Y_{\alpha,\beta}^{A\mp} + Y_{\alpha,\beta}^{B\mp} + Y_{\alpha,\beta}^{C\mp} + Y_{\alpha,\beta}^{D\mp},$$

and

$$Y_{\alpha,\beta}^{A\mp} \equiv S_{\beta,\alpha+1}^{\mp}\binom{\alpha,\beta}{\beta,\alpha}\left(N_\alpha+1\right)\left(f_{\alpha+1}-f_\alpha\right)\left[N_q^{\pm}+\left(1-F_\beta^{\pm}\right)\right],$$

$$Y_{\alpha,\beta}^{B\mp} \equiv -S_{\beta,\alpha+1}^{\mp}\binom{\alpha,\beta}{\beta+1,\alpha+1}\sqrt{\left(N_\alpha+1\right)\left(N_\beta+1\right)}\left(f_{\beta+1}^{\pm}-f_\beta^{\pm}\right)\left[N_q^{\pm}\mp f_{\alpha+1}\right],$$

$$Y_{\alpha,\beta}^{C\mp} \equiv -U_{\alpha,\beta+1}^{\mp}\binom{\beta,\alpha}{\alpha+1,\beta+1}\sqrt{\left(N_\alpha+1\right)\left(N_\beta+1\right)}\left(f_{\beta+1}^{\pm}-f_\beta^{\pm}\right)\left[N_q^{\pm}\pm\left(1-f_{\beta+1}^{\mp}\right)\right],$$

$$Y_{\alpha,\beta}^{D\mp} \equiv U_{\alpha,\beta}^{\mp}\binom{\beta,\alpha+1}{\alpha+1,\beta}\left(N_\alpha+1\right)\left(f_{\alpha+1}-f_\alpha\right)\left[N_q^{\pm}f_\beta^{\mp}\right].$$

With the interacting matrix

$$S_{\beta,\alpha}^{\mp}\binom{k,\eta}{\mu,\nu} \equiv \left[V\left(q_z,q_{\perp 1}^{\mp\beta\alpha}\right)^2\sqrt{\left(q_{\perp 1}^{\mp\beta\alpha}\right)^2+q_z^2}K_{\mu,\nu}^{k,\eta}\left(\frac{r^2}{2}\left(q_{\perp 1}^{\mp\beta\alpha}\right)^2\right)\right]$$

$$+\left[V\left(q_z,q_{\perp 2}^{\mp\beta\alpha}\right)^2\sqrt{\left(q_{\perp 2}^{\mp\beta\alpha}\right)^2+q_z^2}K_{\mu,\nu}^{k,\eta}\left(\frac{r^2}{2}\left(q_{\perp 2}^{\mp\beta\alpha}\right)^2\right)\right],$$

$$U_{\alpha,\beta}^{\mp}\binom{k,\eta}{\mu,\nu} \equiv \left[V\left(q_z,q_{\perp 3}^{\mp\alpha\beta}\right)^2\sqrt{\left(q_{\perp 3}^{\mp\alpha\beta}\right)^2+q_z^2}K_{\mu,\nu}^{k,\eta}\left(\frac{r^2}{2}\left(q_{\perp 3}^{\mp\alpha\beta}\right)^2\right)\right]$$

$$+\left[V\left(q_z,q_{\perp 4}^{\mp\alpha\beta}\right)^2\sqrt{\left(q_{\perp 4}^{\mp\alpha\beta}\right)^2+q_z^2}K_{\mu,\nu}^{k,\eta}\left(\frac{r^2}{2}\left(q_{\perp 4}^{\mp\alpha\beta}\right)^2\right)\right].$$

Acknowledgement

This work was supported by Kyungpook National University Research Fund.

References

1. S. Butscher, F. Milde, M. Hirtschulz, E. Malie, and A. Knorr. *Appl. Phys. Lett*. **91**, 203103 (2007)
2. E. Malie, M. Hirtschulz, F. Milde, Y. Wu, J. Maultzsch, T.F. Heinz, and A Knorr, *Phys. Rev. B* **77**(4), 045432 (2008)
3. C.S. Ting, S.C. Ying, J.J. Quinn, *Phys. Rev. B* **16** 5394 (1977)

4. Xiaoguang Wu, F.M. Peeters, J.T. Devreese, *Phys. Rev. B* **34** 8800 (1986)
5. R. Kubo, *J. Phys. Soc. Jpn*. **12** 570 (1957)
6. J.R. Barker, *J. Phys*. C **6** 2633 (1973)
7. P. Grigoglini, G.P. Parravidini, *Phys. Rev. B* **125** 5180 (1982)
8. H. Mori, *Progr. Theor. Phys*. **33** 423 (1965)
9. V.M. Kenkre, *Phys. Rev. A* **4** 2327 (1971)
10. J.Y. Sug, S.D. Choi, *Phys. Rev. E* **55** 314 (1997)
11. J.Y. Sug, S.D. Choi, *Phys. Rev. B* **64** 235210 (2001)
12. J.Y. Sug, S.H. Lee, *Cent. Eur. J. Phys*. **6** 812 (2008)
13. J.I. Park, H.R. Lee, *Jpn. J. Appl. Phys*. **51** 52402 (2012)
14. J.I. Park, J.Y. Sug, H.R. Lee, *J. Kor. Phys. Soc*. **53** 776 (2008)
15. J.I. Park, H.R. Lee, H.K. Lee, *J. Magnetics* **16** 108 (2011)
16. J.I. Park, *J. Magnetics* **17** 255 (2012)
17. J.I. Park, *Appl. Sci. Converg. Technol.* **29**(4) 82 (2020)
18. T. Dietl, H Ohno: *Mrs Bull*. **28** 714 (2003)
19. S. Chandra, M. Rafiee, J. Doran, and S.J. McCormack, *Sol. Energ. Mat. Sol. C*. **182**, 331 (2018)